

Fig.7 Image processing of tracking two markers for bending angle detection (a matchstick is just for size reference)

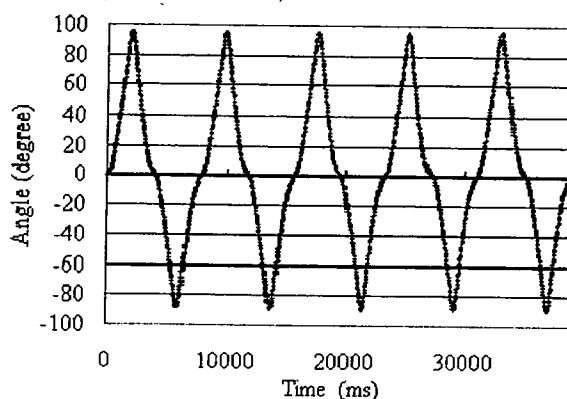


Fig.8 Positioning test for 1 D.O.F bending motion

D. *In vitro* / *in vivo* test

In vitro and *in vivo* tests were performed as shown in Fig.9. In the *in vitro* test, red colored guide laser was irradiated on the surface of a *Macaca fascicularis*'s placenta underwater and the bending angle was changed with the 4-directional switch. The result showed that the laser target point was able to cover the large area of the surface while the manipulator itself is fixed.

For the *in vivo* test, Nd-YAG laser photocoagulation was performed for the mesenteric vessels of a rat. The interrupted blood flow of the photocoagulated vessels was confirmed, which showed that this bending mechanism can deflect the thin fiber of 0.7 mm without damaging it.



Fig.9. *In vitro* and *In vivo* tests (Left: guide laser positioning test for *Macaca fascicularis*'s placenta underwater (*in vitro*), Right: laser photocoagulation test for the mesenteric vessels of a rat (*in vivo*))

E. Discussion

Good performance of the developed manipulator was confirmed in the *in vivo* test. When the manipulator was controlled with the switch under the direct vision of the target,

the operator easily controlled the tip of the manipulator to his/her target point. Improvement of the positioning accuracy will enable the combination of the manipulator and navigation systems using endoscopic image, ultrasound or MRI data.

On the other hand, problems with the handheld manipulator interface were observed. When operators were allowed to move the manipulator around a trocar while controlling bending motion, they found it difficult to combine all movements to position the manipulator's tip as they want. This problem was remarkable when the target area was placed upper side. Another problem is the stagger caused by the pushing the switch when the switch is attached to the manipulator. Handheld manipulators such as [12] are studied since the interface is expected to reduce the cost and be familiar for surgeons, but its usability needs further study.

IV. VISCOELASTIC MODEL OF FETAL RAT TISSUE

A. Goals

Fetal tissue is described by surgeons as soft, fragile, gelatinous, and difficult to handle. The fragility is one of the technical difficulties of fetal surgery. However, the overall mechanical properties of fetal tissue have rarely studied. To establish fetal model based on its properties is important for developing surgical robots such as a robotic patch stabilizer in Fig.2 because the precise and delicate force control will be necessary. Some studies insist that robotic force control using organ model is important for handling soft organs [24,25].

In the following, the shear creep tests for fetal rat tissue are reported and a viscoelastic model is proposed. Brain, lung and liver tissues of an adult rat are also tested under the same test conditions to illustrate the unique features of fetal rat tissue.

B. Methods

Shear creep tests were conducted for the fetal rat tissue of 16 to 20 days gestation (Wistar rat: usually born at 21 to 22 days gestation). A circular test piece of 8 mm in diameter was cut out from the abdominal wall of each fetal rat. The abdominal wall was chosen as a test piece to avoid the influence by growing (hardening) bones. The back skin of the fetal rat would be better as a test piece, but the skin was too thin to perform the creep tests.

A rheometer (AR550, TA-Instrument, New Castle, DE, USA) was used to perform creep tests at 0.1, 0.2, 0.3, 0.4, 0.5 kPa and 5 minutes for loading and 5 minutes for relaxing. 0.05, 0.075, 0.1kPa were loaded to the fetal tissue of 16 days gestation since it fractured around 0.2 to 0.4 kPa. The test piece was placed on a piece of sandpaper attached to the specimen tray to fix the test piece in position. The test piece was then pressed by a geometry plunger (8 mm in diameter) to 0.1 N then shear stress was loaded. A piece of sandpaper is also attached to the tip of the plunger for avoiding slip. Saline water at 36 °C was filled in the specimen tray to simulate intrauterine environment. These tests were performed within 12 hours after the sample resection.

All experimental procedures were performed according to our institutional animal ethics guidelines, which are based on those of the National Institutes of Health of USA.

C. Results

The creep compliance of fetal rats (16 days at 0.1 kPa, 17-20 days at 0.5 kPa), adult rat brain(0.3 kPa), adult rat lung(0.5 kPa), and adult rat liver(0.5 kPa) was shown in Fig. 10. Although the stress dependence was observed, all test results showed viscoelastic properties with the features of instantaneous deformation, retardation and residual strain.

The initial creep compliance represents the instantaneous deformation due to the elasticity of the tissue. The gradual increase represents the time-dependent deformation change due to the viscosity of the tissue.

This result showed the big change of fetal tissue property from 18 days to 19 days in gestations. In visual observation, the fetal tissue is gelatinous before 19 days. It is known that human fetal tissue property is also dramatically changed around 19 weeks in gestation. The equivalent age of human fetus is unknown, it is supposed that so-called gelatinous human fetal tissue is similar the fetal rat tissue before 19 days in gestation.

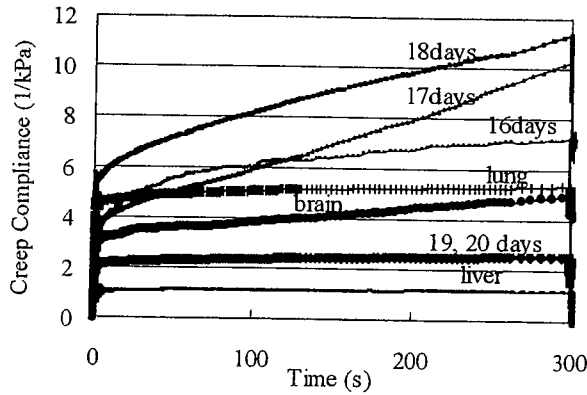


Fig. 10. Creep compliance of fetal rats (16 days at 0.1kPa, 17-20 days at 0.5kPa), adult rat brain(0.3kPa), adult rat lung(0.5 kPa), and adult rat liver(0.5 kPa).

D. Viscoelastic Model

As the first step toward establishing a fetal rat model, the four element model (Burger’s model) was used to compare the fetal rat tissue with other soft organs. The four element model is often used for modeling biomaterials and it is expressed with the combination of the Maxwell model and Voigt model as shown in Fig. 11. The creep compliance behavior of the model is expressed in (3) and (4), where J is creep compliance, G_m is elastic coefficient of Maxwell element, η_m is viscous coefficient of Maxwell element, G_v is elastic coefficient of Voigt element, η_v is viscous coefficient of Voigt element, τ is shear stress and U is step input.

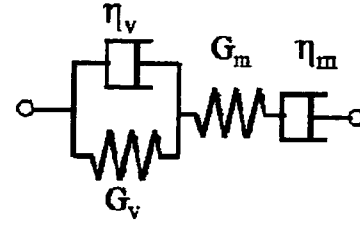


Fig. 11. Four element model (Burger’s model) for viscoelastic materials

$$J(t) = \left[\frac{1}{G_m} + \frac{1}{\eta_m} \cdot t + \frac{1}{G_v} \cdot \left\{ 1 - \exp\left(-\frac{G_v}{\eta_v} \cdot t\right) \right\} \right] \cdot [U(t)] \quad (3)$$

$$\tau(t) = \tau_0 \cdot [U(t)] \quad (4)$$

The results of the experiments showed in Fig.10 were fitted to the four element model to figure out the parameter values. The identified coefficient values of each material are shown in Table I.

Table I. Identified coefficient values of the four element model

	Gm	hm	Gv	hv	SSE
16 days	0.3	0.7	7.1E-05	0.7	13.1
17 days	0.3	4.8	-7.1E-05	5.4	1.5
18 days	0.2	11.0	1.6E-02	15.9	2.8
19 days	0.5	23.5	5.4E-03	25.0	0.1
20 days	0.5	24.6	7.2E-03	26.3	0.1
brain	0.3	11.8	2.2E-03	13.0	0.9
lung	0.2	13.1	4.2E-03	14.1	0.7
liver	1.0	9.5	4.8E-04	9.6	0.1

E. Discussion and Future works

The identified coefficient value demonstrates the differences between materials. Low elasticity and low viscosity are unique features of fetal tissue and its behavior is totally different from other soft tissues.

Low elasticity and low viscosity means that the tissue is easy deformable and its difficult to keep a constant stress on it. The robotic patch stabilizer in Fig.2 needs to touch a fetus during surgery while keeping adequate force on it because the patch and the fetus must be in contact. The unique features of fetal tissue require precise force control of the robotic patch stabilizer to keep the close contact on it. Since it is supposed to be very difficult for surgeons to control the force while controlling the bending laser manipulator in the procedure in Fig.2, semi-automatic or automatic force control will be useful.

For the future works, the fabrication of fetal phantoms having the similar mechanical properties of fetal rat is in process. A prototype of the robotic patch stabilizer (2.4mm in diameter, 2 D.O.F) has been developed using the same bending mechanism as shown in Fig.12. We have confirmed that the force on the tip of the stabilizer is estimated by measuring wire tension, the next step is to develop a force control method using the fetal phantom.



Fig. 12. A prototype of the robotic patch stabilizer

V. CONCLUSION

The feasibility of the developed bending laser manipulator was confirmed *in vivo*. Further improvement of the positioning accuracy using wire tension sensors is future work to achieve the combination of the manipulator and navigation systems. The evaluated features of fetal rat tissue and the proposed viscoelastic model will lead to the development of a fetal phantom and a force control method of the robotic patch stabilizer or other robotic applications.

ACKNOWLEDGMENT

A placenta of *Macaca fascicularis* was kindly provided from Non-human Primate Reagent and Resource Program in Tsukuba Primate Research Center, National Institute of Biomedical Innovation.

REFERENCES

- [1] Danzer E, Sydorak RM, Harrison MR, Albanese CT. , "Minimal access fetal surgery", *Eur J Obstet Gynecol Reprod Biol*, 2003 May 1, 108(1), pp.3-13
- [2] Senat MV, Deprest J, Boulvain M, Paupe A, Winer N, Ville Y, "Endoscopic laser surgery versus serial amnioreduction for severe twin-to-twin transfusion syndrome", *N Engl J Med*. 2004 Jul 8, 351(2), pp. 182-4
- [3] N.Tulipan, "Intrauterine closure of myelomeningocele : an update", *Neurosurgery Focus*, February 2004, Vol.16, pp1-4
- [4] Kanako Harada, Kentaro Iwase, Kota Tsubouchi, Kousuke Kishi, Tetsuya Nakamura, Toshio Chiba, Masakatsu G.Fujie, "Micro manipulator and Forceps Navigation for Endoscopic Fetal Surgery", *J of Robotics and Mechatronics*, Vol.18, No.3, 2006, pp.257-263
- [5] Kohl T, Hering R, Heep A, Schaller C, Meyer B, Greive C, Bizjak G, Buller T, Van de Vondel P, Gogarten W, Bartmann P, Knopfle G, Gembruch U. , "Percutaneous fetoscopic patch coverage of spina bifida aperta in the human--early clinical experience and potential", *Fetal Diagn Ther.* ,2006,21(2),pp.185-93
- [6] Enosawa S, Tanemoto T, Harada K, Ide A, Tsubouchi K, Fujie M, Takezawa T, Chiba T. , "Vitrified collagen sheet, Vitrigel, a novel biophilic sealant for fetal surgery", *The 25th Annual Meeting of International Fetal Medicine and Surgery Society (IFMSS2006)*
- [7] Kevin Cleary, Charles Nguyen, "State of the Art in Surgical Robotics: Clinical Applications and Technology Challenges", *Comput Aided Surg*. 2001,6(6), pp.312-28
- [8] O. S. Aaronson, N. B. Tulipan, R. Cywes, H. W. Sundell, G.H. Davis, J. P. Bruner, and W. O. Richards, "Robot-Assisted Endoscopic Intrauterine Myelomeningocele Repair: A Feasibility Study," *Pediatric Neurosurgery*, 2002., Vol.36, pp. 85-89
- [9] T. Kohl et al., "Percutaneous fetoscopic patch coverage of experimental lumbosacral full-thickness skin lesions in sheep," *Surgical Endoscopy*, Vol.17, 2003, pp. 1218-1223.
- [10] Knight CG, Lorincz A, Johnson A, Gidell K, Rabah R, Klein MD, Langenburg SE, "Robot-enhanced fetoscopic surgery", *J Pediatr Surg*. 2004 Oct, 39(10), pp.1463-5
- [11] J. Furusho, T. Katsuragi, T. Kikuchi, T. Suzuki, H. Tanaka, Y. Chiba, H. Horio, "Curved multi-tube systems for fetal blood sampling and treatments of organs like brain and breast", *International Journal of Computer Assisted Radiology and Surgery*, Vol.1, Supplement 1, June 2006, pp.223-226
- [12] H. Yamashita, K. Matsumiya, K. Masamune, H. Liao, T. Dohi, T. Chiba, "Two-DOFs bending forceps manipulator of 3.5-mm diameter for intrauterine fetus surgery: feasibility evaluation", *International Journal of Computer Assisted Radiology and Surgery*, Vol.1, Supplement 1, June 2006, pp.218-220
- [13] K.Oka, T.Nakamura, K.Harada, Y.Ohkawa, T.Hidaka, T.Chiba, "Development of laser forceps for fetal surgical treatment", *Proc. of IFMBE World Congress on Medical Physics and Biomedical Engineering (WC2006)*, pp.2976-2979
- [14] Anna Eisenberg, Oliver Tonet, Paolo Dario, Giovanna Macri, Maria Chiara Carrozza, "Microfabricated instrument for haptic tissue recognition in fetal cardiac surgery", *The First IEEE/RAS-EMBS International Conference on Biomedical Robotics and Biomechanics (BioRob 2006)*, pp.1183 - 1188
- [15] Pietro Valdastri, Kanako Harada, Arianna Menciassi, Lucia Beccai, Cesare Stefanini, Masakatsu G Fujie, Paolo Dario, "A Three Components Force Sensorized Tip for Minimal Invasive Surgery and Catheterism", *IEEE Transaction on Biomedical Engineering*, Volume 53, Issue 11, 2397 -2400, 2006 - Nov.
- [16] Wataru Makishi, Tadao Matunaga, Yoichi Haga, Masayoshi Esashi, "Active Bending Electric Endoscope Using Shape Memory Alloy Coil Actuators", *Proc. of the 1st IEEE/RAS-EMBS 2006 International conference on Biomedical Robotics and Biomechanics (Biorob2006)*, pp.217-219
- [17] Nakamura R, Oura T, Kobayashi E, Sakuma I, Dohi T, Yahagi N, Tsuji T, Shimada M, Hashizume M, "Multi-DOF Forceps Manipulator System for Laparoscopic Surgery - Mechanism miniaturized & Evaluation of New Interface -" *Proc. of Fourth International Conference on Medical Image Computing and Computer assisted Interventions (MICCAI2001)*, pp.606-613
- [18] K. Nishizawa, and K. Kishi, "Development of Interference-Free Wire-Driven Joint Mechanism for Surgical Manipulator Systems," *Journal of Robotics and Mechatronics*, Vol.16, No.2, pp. 116-121, 2004
- [19] Makoto Jinno, Takamitsu Sunaoshi, Toyomi Miyagawa, Takehiro Hato, Nobuto Matsuhira, Yasuhide Morikawa, Soji Ozawa, Masaki Kitajima, "Development of Robotic Forceps for Laparoscopic Surgery", *Journal of Robotics and Mechatronics*, Vol.18, No.3, 2006, pp.249-256
- [20] Koji Ikuta, Daisuke Yajima, Hironobu Ichikawa, Katsuya Suzuki, "Hydrodynamic Active Catheter with Multi Degrees of Freedom Motions", *Proc. of IFMBE World Congress on Medical Physics and Biomedical Engineering (WC2006)*, pp.2968-2971
- [21] Yoriko Iwamori, Jun Okamoto, Masakatsu G.Fujie, "Multi-DOF Forceps Manipulator for an Approach to the Dorsal Aspect of an Organ", *Proc. of IFMBE World Congress on Medical Physics and Biomedical Engineering (WC2006)*, pp. 4022-2026
- [22] Wei Wei, Kai Xu, Simaan, N., "A Compact Two-armed Slave Manipulator for Minimally Invasive Surgery of the Throat", *The First IEEE/RAS-EMBS International Conference on Biomedical Robotics and Biomechanics (BioRob 2006)*, pp.769 - 774
- [23] Gravagne, I.A., Rahn, C.D., Walker, I.D., "Large deflection dynamics and control for planar continuum robots", *Mechatronics*, IEEE/ASME Transactions on Volume 8, Issue 2, June 2003, pp.299 - 307
- [24] Yoshizawa, A., Jun Okamoto, Yamakawa, H., Fujie, M.G. "Robot Surgery based on the Physical Properties of the Brain - Physical Brain Model for Planning and Navigation of a Surgical Robot-", *Proc. of the 2005 IEEE International Conference on Robotics and Automation (ICRA 2005)*, pp.904 - 911
- [25] Yo Kobayashi, Jun Okamoto, Fujie, M.G., "Physical Properties of the Liver and the Development of an Intelligent Manipulator for Needle Insertion", *Proc. of the 2005 IEEE International Conference on Robotics and Automation (ICRA 2005)*, pp.1632 - 1639

永瀬 優子¹, 若林 洋明¹, 望月 剛¹, 原田香奈子², 千葉 敏雄², 中村 充一³,
伊関 洋³, 佐久間一郎⁴

¹アロカ(株), ²国立成育医療センター, ³東京女子医科大学 先端生命医科学研究所,
⁴東京大学 大学院工学系研究科

【目的】

胎児治療を安全にかつ正確に行なう方法として、超音波ナビゲーションが必須の手段となりつつある。本研究では双胎間輸血症候群の治療を具体例として、内視鏡や鉗子の誘導を目的とし、すなわち、超音波3次元エコーデータを手術中に収集し、このデータをもとに、子宮内での内視鏡や鉗子の位置を実時間で観察できる。また、この位置情報から、胎児や胎盤組織への接触を未然に知らせる警戒通知可能な、システムを構築する。本発表では、このシステムの超音波ナビゲーションシステムの位置精度を実験から明らかにし、システムの有効性を述べる。

【方法】

図1には光マーカ付き超音波3Dプローブと4つの硬球ターゲットをもつ超音波エコー精度測定治具の写真を示す。超音波3次元プローブに取り付けられた複数の光マーカは超音波3次元プローブの3次元位置を計測するためのものである。別の位置に設置された赤外線カメラが、自分の位置を原点とするワールド空間座標上で光マーカの3次元位置を計測する。一方、超音波プローブは治具の4つの硬球ターゲットからのエコーを含む3次元エコーデータを収集する。これら光学系と超音波系により得られた各データを総合すると、4つの硬球のワールド空間上の位置(座標)が計算される。この値と実際の位置(座標)との比較から、光-超音波系の計測時の総合誤差を求めることが可能である。実際を想定し測定ごとに、(1)超音波プローブへの光マーカの着脱、(2)超音波プローブの硬球治具への設置、(3)超音波プローブ駆動系のリセット、かつ、(4)治具の位置を光位置計測範囲内の異なる位置へ移動を行ない、光-超音波系総合の計

測により、4つの硬球のワールド空間上の座標を求めた。この計測を10回試行し、これを1セットとして、2セット行なった。

【結果】

表1に超音波と光学系の両方を含む総合的な誤差の結果を示す。2回のセット間での差は0.6mm以内であることから、測定に関する再現性が良いことが分かる。また、誤差には、x, y, zの方向により違いがあること、さらに詳細な測定データの分析により、超音波系の誤差は超音波3Dプローブの機械系に依存する誤差が大きいこと、超音波系と光学系とは独立であるために、両者の誤差が蓄積、または打ち消しあう状況があることなどが分かった。発表ではこの詳細な結果を報告すると同時に、本システムの応用例を示す。



図1 光マーカ付き超音波3Dプローブと4つの硬球ターゲットをもつ超音波エコー精度測定治具

表1 4点の硬球ターゲットのワールド空間座標での計測値と実際の誤差

硬球4点の位置の平均 (10サンプル)	1セット (10サンプル)	2セット (10サンプル)
	誤差 [mm]	誤差 [mm]
X座標値	0.33	0.9
Y座標値	3.05	2.5
Z座標値	2.25	2.5

Accuracy of Positioning in Ultrasound Navigation System for Fetal therapy

Yuko NAGASE¹, Hiroaki WAKABAYASHI¹, Takashi MOCHIZUKI¹, Kanako HARADA², Toshio CHIBA², Ryoichi NAKAMURA³, Hiroshi ISEKI³, Ichiro SAKUMA⁴

¹ALOKA Co., Ltd., ²National Center for Health and Development, Tokyo, Japan,

³Department of Advanced Biomedical Engineering and Science, Tokyo Women's Medical University, Tokyo, Japan,

⁴School of Engineering, The University of Tokyo, Tokyo, Japan

胎児外科治療におけるレーザー照射量制御

- 熱電対を用いた in vivo 実験について -

Laser Irradiation Power Control for Fetal Surgical Treatment

- In-vivo experiment used thermocouple -

○長縄明大 (秋田大学), 鈴木克征 (秋田大学),
 岡潔 (日本原子力研究開発機構), 中村哲也 (ペンタックス株式会社),
 植田裕久 (ペンタックス株式会社), 妻沼孝司 (株式会社フジクラ),
 千葉敏雄 (国立成育医療センター), 森戸義美 (株式会社関電工)

○Akihiro NAGANAWA, Akita University, 1-1 Tegata-gakuen-cho, Akita-shi, Akita
 Katsuyuki SUZUKI, Akita University, 1-1 Tegata-gakuen-cho, Akita-shi, Akita
 Kiyoshi OKA, Japan Atomic Energy Agency, 2-4 Shirane, Shirakata, Tokai-mura, Naka-gun, Ibaraki
 Tetsuya NAKAMURA, PENTAX Corporation, 1-9-30 Shirako, Wakou-shi, Saitama
 Hisahiro UEDA, PENTAX Corporation, 2-36-9 Maeno-cho, Itabashi-ku, Tokyo
 Koji TSUMANUMA, Fujikura Ltd., 1440, Mutsuzaki, Sakura-shi, Chiba
 Toshio CHIBA, National Center for Child Health and Development, 2-10-1 Ohkura, Setagaya-ku, Tokyo
 Yoshimi MORITO, Kandenko Co., Ltd., 4-8-33 Shibaura, Minato-ku, Tokyo

Key Words : Fetal surgical treatment, Composite-type optical fiber, Temperature control,
 Blood-flow interception

1. 緒言

一絨毛膜二羊膜性双胎では、二人の胎児が臍の緒、血管を介して一つの胎盤につながっており、胎盤上の無数の血管の中の何本かは吻合血管である。通常、二人の間の血液の流れは、吻合血管を通してお互いを行き来しているが、この血液の流れのバランスが崩れると、一方の胎児が血液過剰の状態 (受血児)、もう一方の胎児が血液過少の状態 (供血児) となる。これを双胎間輸血症候群という⁽¹⁾。双胎間輸血症候群では、重症の場合、受血児・供血児ともに子宮内胎児死亡や新生児死亡となる危険が高く、また母体も羊水が過剰に増加し、これが原因で流産・早産となることがある。

近年、双胎間輸血症候群に対して、胎盤表面の吻合血管を内視鏡で観察しながらレーザーで焼灼して閉塞し、双胎間の血流を分離する治療が行われている。しかし、これまでの内視鏡装置では、血管表面とレーザーファイバ先端間距離を適切に保つことが必ずしも容易ではなく、またレーザーの出力値や照射時間、血流遮断の状況は医師の経験や直感に依存しているのが現状である。

そこで著者らは、焼灼用レーザーファイバを観察用ファイバの中心に配置した複合型光ファイバを用いたレーザー治療装置の研究開発を行っている⁽²⁾。本装置では、常に視野中心に血管を捉えながら正確なレーザー照射を行えるだけでなく、距離計測を行うことができ

るためビームウエスト部での焼灼が可能であり、さらにレーザードップラー方式の血流計測装置を組み込んでいるため工学的に血流遮断を評価することができる⁽³⁾。これまで豚レバーに対してレーザー照射部の温度管理を行いながらレーザー出力の制御を行ってきた⁽⁴⁾が、本研究ではその効果を実際の血流で評価するため、豚の腸間膜血管に対して行った in vivo 実験の結果について述べる。

2. 複合型光ファイバシステム

複合型光ファイバシステムは、光ファイバスコープ、レーザー発生装置、カップリング装置、PCなどで構成されている。Fig. 1は、焼灼用レーザーファイバを画像用ファイバの中心に配置した複合型光ファイバを示しており、写真(a)はファイバ先端を示している。焼灼レーザーの光ファイバ径は $\phi 0.1\text{mm}$ に細径化し、その周囲に画像伝送用光ファイバを、さらに照明光を伝送す

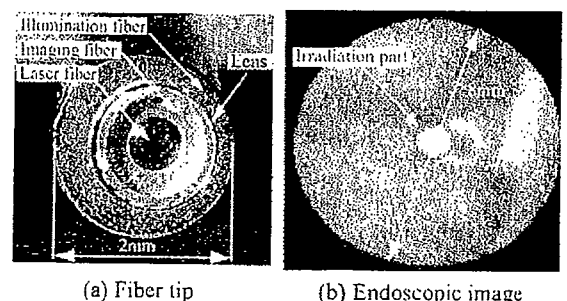


Fig. 1 Composite-type optical fiberscope

るための光ファイバを周囲に一体化しつつ全体外径を ϕ 2mm とした。ファイバ先端には、レーザーを集光させ、また内視鏡画像の視野を広げるためのレンズが取り付けられている。レーザーは、IPG 製の Yb(イッテルビウム) ファイバーレーザー (発振波長は 1075nm) を使用している。(b) は内視鏡画像を示しており、直径約 8mm の視野の中心にレーザー照射部が見られる。レーザー照射は、PC により 0~50W をリアルタイムで調整できる。

3. 実験システム

Fig. 2 は、実験装置の構成を示している。本実験は、豚の腸間膜を開いて太さ約 0.5mm の静脈血管を取り出し、その血管を容器で囲み、常温の水を入れた in vivo 実験により行った。温度管理のための熱電対は、レーザーによる破損を防ぐため照射部より 1mm 下流の血管表面に設置し、センサ回路を介して照射部の温度情報を PC 内にフィードバックする。PC では、目標温度との偏差に基づき、PID コントローラにより適切な指令をレーザー装置に送り、レーザーの出力を制御して温度管理を行う。なお、本実験では、血管表面とファイバ先端間距離を 9mm とした。

4. 実験結果

Fig. 3 は、温度管理の結果を示している。本実験では、目標温度は 60℃ とし、制御時間は 20sec、レーザー出力の上限は 20W に設定した。図より、レーザー照射が開始されると同時に温度が上昇しはじめ、照射開始から約 8 秒後に目標温度 60℃ に到達していることがわかる。また、目標温度 60℃ に到達した後も ± 1.5 ℃ 以内の精度で温度を保持できており、このときのレーザー出力は約 10W であった。これらの実験結果より、本制御システムでは適切な温度管理を実現できるといえる。

Fig. 4 は、照射後の血管の外観を示している。レーザー照射部においては血管が白く熱収縮しており、太さ約 0.5mm の血管の上流部には、血流が遮断されたこ

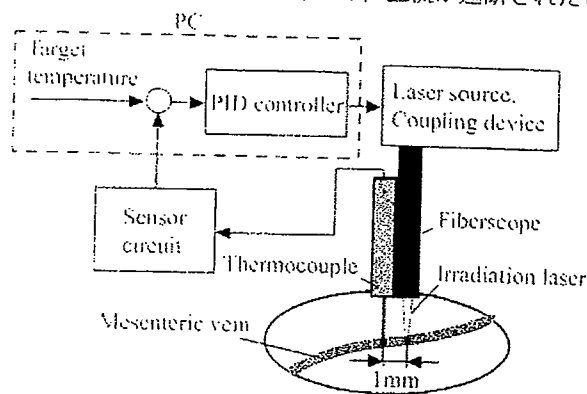


Fig. 2 Experimental system

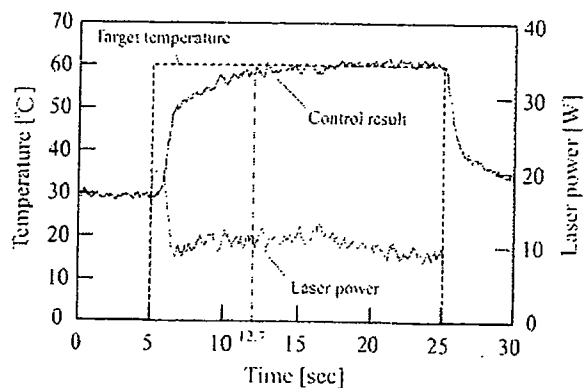


Fig. 3 Experimental result

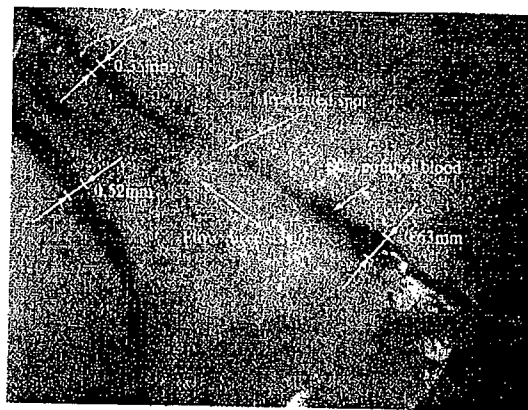


Fig. 4 Photograph of irradiated spot

とによる最大 0.63mm の血液の停留点が見られた。なお、下流部は血流が遮断されたことにより、血管の太さは 0.35mm となった。また、Fig. 4 の撮影後、照射部より下流の血管を切ったところ、血液が流れ出なかったため、血流は完全に遮断されていたことを目視により確認した。

5. 結言

本研究では、レーザー照射部の温度管理を行いながら血流を遮断するために熱電対を用いたフィードバック制御系を構成し、in vivo 実験を行ったところ、良好な結果が得られた。今後の課題としては、太さの異なる血管や目標温度の設定、照射時間の検証などが挙げられる。

参考文献

- (1) 千葉, 北川, 左合, 林, 松岡: 一絨毛膜性双胎と胎児外科治療 (1), 産科と婦人科, 71-10, pp.1359-1366, 2004.
- (2) K. Oka, T. Nakamura, K. Harada, Y. Ohkawa, T. Hidaka and T. Chiba, "Development of laser forceps for fetal surgical treatment", World Congress on Medical Physics and Biomedical Engineering, pp.2976-2979, 2006.
- (3) 岡, 中村, 植田, 鳥谷, 妻沼, 長縄, 渡邊, 石山, 山下, 千葉: TTTS に対する FLPC のためのレーザー内視鏡の高機能化, 第 5 回日本胎児治療学会学術集会, 2007 年発表予定.
- (4) 長縄, 関, 岡, 千葉, 中村, 市倉, 森戸: 双胎間輸血症候群における胎児鏡レーザー照射制御, 計測自動制御学会第 7 回適応学習制御シンポジウム資料, pp.29-32, 2007.



SMIT 2007 Program

Touch the future of medical technology.

第十九回
先端医療
技術学会
大会

Date: 20-22 November 2007

Sendai, Japan

**The 19th
International Conference of
Society for Medical Innovation
and Technology**

"Practice meets technology. Technology meets practice."

is an efficient diagnostic tool in the evaluation of abdominal aneurysms and dissections and can be considered the modality of choice in case of aortic branches involvement.

JS1-6

Thoracoscopic thymectomy using high vision flexible thoraco-videoscope

Hisashi Iwata, Koyo Shirahashi, Shinsuke Matsumoto, Hirofumi Takemura
General and Cardiothoracic Surgery, Graduate School of Medicine, Gifu University, Japan

Purpose: Recently, thoraco-videoscopic surgery for anterior mediastinal diseases is generally performed. We performed assisted thoracoscopic surgery (both direct vision and thoraco-videoscopic vision) for mediastinal solid tumors such as thymoma. We also performed complete thoracoscopic surgery (only thoraco videoscopic vision) such as extended thymectomy for myasthenia gravis using high vision flexible thoracoscopy. High vision flexible thoraco-videoscope (CAT No. R1443UB, Olympus, Japan) provides a phenomenal 1080 effective scanning lines of picture formation, and delivers picture quality that is more than twice as good as conventional videoscope. **Methods:** Our indication for complete thoracoscopic extended thymectomy is case without thymoma, with appropriate thoracic cavity for working space and fat tissue, under the informed consent of patients. Briefly, we used two 2cm ports at fourth and fifth intercostal space of anterior and middle axillar line with Osaka university sternum elevation method. Cervical incision and another port at fifth intercostal space of middle clavicular line are used in some case. **Result:** We performed thymectomy in 11 cases during 2 years. Six cases were thymoma including 2 cases of myasthenia gravis. We performed assisted thoracoscopic thymo-thymectomy in all cases. Thoraco- videoscopic vision was useful to understand the phrenic nerve to preserve. We planed complete thoracoscopic extended thymectomy in 5 cases. One case was contra-indication of ours due to high volume of fat tissue. One converted to conventional procedure by median sternotomy due to intra-thoracic adhesion. In one case, we used the high vision flexible thoraco-videoscope. High vision field made tissue detail clear and safe to perform operation in the thoracic cavity. There were no serious complications. **Conclusion:** Our surgical procedure using both assisted and complete thoraco-videoscope was useful, in particular with the high vision flexible thoraco-videoscope to make tissue detail clear.

JS1-7

Composite-type optical fiberscope for laser surgery for Twin-to-twin Transfusion Syndrome (TTTS)

Tetsuya Nakamura¹, Kiyoshi Oka², Hiromasa Yamashita³, Hirohisa Ueda¹, Toshio Chiba³

¹Incubation Center, Research & Development Headquarters, PENTAX Corporation, Japan,

²Quantum Beam Science Directorate, Japan Atomic Energy Agency, Japan,

³Department of Strategic Medicine, National Center for Child Health and Development, Japan

Introduction: In fetoscopic laser photocoagulation of placental communicating vessels for twin-to-twin transfusion syndrome (TTTS), there are several technical issues. These

include; 1) laser light diffusion that reduces the energy density, 2) unknown distances between the placental surface and laser fiber tip and 3) difficulties in assessing actual flow of the targeted blood vessels. To settle these problems, we successfully developed a new small composite-type optical fiberscope. Device specifications: Our optical fiberscope (diameter: 2.2 mm) consists of a couple of collecting lenses (focal length: 10 mm) and coaxially arranged two types of optical fibers, one is a centrally located single fiber for laser ablation and the other is surrounding bundle of fibers for fetoscopic image. Furthermore, the fiberscope has two vital functions, one is a distance measurement based on a reflective light intensity and the other is a blood flow measurement using the laser Doppler method. **Experimental results:** We irradiated underwater porcine liver using our system and the current devices and compared the ablation spots (gross appearance, diameter and depth) with various conditions (irradiation energy: 10~40 W, distance between the fiber tip and the tissue: 5~20 mm). Changes in laser energy didn't affect the size of ablation parts if the fiber tip was set 10-mm apart from the tissue. Next using anesthetized pigs, we tested the accuracy of the distance measurement and blood flow assessment before/after underwater mesenteric vessel irradiations. We could measure both the distance to the target and the blood flow in real-time with minimal errors. **Conclusion:** Based on minimally-required laser energy presented intraoperatively by our new system, we may be able to achieve much less invasive but adequate ablation of the vessels responsible for TTTS. Additionally, this system is expected to serve as a useful hemodynamic monitoring device for the target vessels.

Joint Symposium 2 (JSES/SMIT): Endoluminal surgery and NOTES

JS2-1 (Keynote Lecture)

Options and solutions for endoluminal and transluminal surgery

Gerhard Buess

Division of Minimally Invasive Surgery, Department of general surgery, Tübingen University, Germany

No Abstract

JS2-2

Endoluminal fundoplication using the EsophyX

Marco Maria Lirici¹, Odette Hasaj², Flora Salerno¹, Andrea Califano¹

¹Department of General and Thoracic Surgery, BMM Hospital Reggio Calabria, Italy,

²S. Anna Hospital - Catanzaro

Gastroesophageal reflux is a common digestive tract disease. GERD can lead to a variety of complications. Due to the high prevalence of the disease and in order to prevent its complications, a proper treatment is mandatory: proton pump inhibitors being the most common therapy. Unfortunately medications do not prevent reflux. In serious cases and in non responding patients laparoscopic fundoplications may be indicated. Unfortunately, laparoscopic fundoplication still presents significant risks. A new endoluminal option is now available to treat GERD: Endoluminal Fundoplication using the Esophyx (Endogastric Solution) device. The procedure is still under evaluation. The first case of ELF by Esophyx

performed at the Department of General Surgery of the BMM Hospital is here reported. The patient signed an informed consent form. Feasibility of the procedure is confirmed by preoperative endoscopy. The procedure is carried on under general anaesthesia with naso-tracheal intubation. Patient is positioned on the left side. The EsophyX device is placed over a 10 mm gastroscope, inserted transorally and advanced into the stomach. The z-line is visualized through the window in the EsophyX shaft. Vacuum suction is created to hold the esophagus while advancing the device till the z-line is at the level of diaphragm, thus reducing the hiatal hernia. Once the stomach and the esophagus are in the correct position, an elyca retractor is deployed to engage stomach tissue and pulled. A serosa-to-serosa flap tissue is created and drawn into the tissue mold and locked in place. Polypropylene fasteners are delivered across this flap (the future wrap to be created around the cardias) using a stylet to penetrate the tissue and a pusher to advance them. The serosa-to-serosa plication (240 degree) is created by firing around 12 to 14 fasteners. Postoperative course was uneventful, the patient discharged on postop day 2. Early follow-up showed symptoms reduction.

JS2-3

Percutaneous endoscopic intragastric surgery (PEIGS) in the treatment of gastric SMT located close to the esophago-gastric junction

Takahiro Kinoshita¹, Eiji Kanehira², Ryoji Kato¹

¹Department of Endoscopic Surgery, Toho University Sakura Medical Center, Japan,

²Minimally Invasive Surgery Center, Yotsuya Medical Cube, Tokyo, Japan

With better technical advances, an increasing number of gastric SMT including gastrointestinal stromal tumors (GISTs) are being resected laparoscopically using stapling devices. However, for SMTs of intraluminal growing type near the esophago-gastric junction (EGJ) laparoscopic wedge resection is impossible because of the fear of postoperative stenosis. For these cases, endoluminal surgical approach appears to be most suitable. Percutaneous endoscopic intragastric surgery (PEIGS) is categorized within endoluminal surgery. In PEIGS three cannulae are inserted percutaneously into the gastric cavity, using a gastropexy device. The gastric cavity is dilated by CO₂ insufflation and full-thickness resection including the tumor is carried out using a grasper and a high-frequency hook under percutaneous endoscopic view. With endoluminal view, we can clearly recognize the tumor capsule to perform more accurate resection. After the irrigation with saline solutions, the full-thickness defect is closed by endoscopic suturing. For the patients with intraluminal growing SMTs located close to EGJ, PEIGS can be the most beneficial therapy, though those candidates are very limited. In this paper, we will present its technique.

JS2-4

Achievement to advanced intrauterine fetal surgery with endoscopic miniature bending manipulator

Hiromasa Yamashita¹, Kiyoshi Matsumiya², Ken Masamune², Hongen Liao³, Toshio Chiba¹, Takeyoshi Dohi²

¹Department of Strategic Medicine, National Center for Child Health and Development, Japan,

²Graduate School of Information Science and Technology, The University of Tokyo, Japan,

³Graduate School of Engineering, The University of Tokyo, Japan

Purpose: We present the endoscopic miniature manipulator (3.5-mm in diameter) with two degrees of freedom (DOFs) bending mechanism for less invasive intrauterine fetal surgery. This manipulator is useful especially for intrauterine myelomeningocele repair (IUMR), twin-to-twin transfusion syndrome (TTTS) and so on. **Methods:** Our miniature manipulator has bending mechanism controlled by the original wire-guided linkage driving method to realize its miniaturization with a central channel. Our 2-DOFs (horizontal/vertical) bending mechanism performs an accurate manipulation and a large bending angle between ± 90 degrees. And to mount a couple of different functions (grasping, shearing, laser irradiation) for diverse surgical procedures, the end-effector modules are easily replaceable. In addition, the manipulator has, like other surgical tools, a grip-type interface for single-hand control. The tip side of the manipulator is detachable freely from the actuators and interface side for easy cleaning and autoclave. Worthy of note, the manipulator does not weigh much, approximately 500 grams. **Results:** The manipulator revealed high bending accuracy in positioning with a minimal error of 0.1 mm, large bending force of maximum 2.57 N (262 gf) and gasping force of maximum 3.48 N, (355 gf). In phantom experiment with intrauterine fetus model using two manipulators, we were able to hand over the suture needle from one hand to another hand underwater condition with only endoscopic view. And in laser photocoagulation test with laser fiber, the manipulator performed less irradiation energy loss with large bending angle up to 80 degrees. Furthermore we ablated surface of underwater chicken liver successfully. **Conclusion:** Our new manipulator has high mechanical performance irrespective of bending dimensions and/or orientations. This robotized manipulator is sure to serve as a "new hand" for future advanced fetal surgery with an introduction of "new eyes", that are navigation system and small 3D scope.

JS2-5

A creation of gastric orifice using double-straight needle device for the pre-stage of natural orifice transluminal endoscopic surgery

Nobumi Tagaya, Mitsuru Ishizuka, Keiichi Kubota

Second Department of Surgery, Dokkyo Medical University, Japan

Natural orifice transluminal endoscopic surgery (NOTES) is currently studied as a potentially less invasive alternative to conventional laparoscopic abdominal surgery. However, the issue associated with the creation of gastric orifice is still unsolved. Before applying NOTES, we introduce the simple method for opening and closing the gastric wall using a double-straight needle device under the assistance of 3-mm miniaturized instruments. Animal models were anesthetized and peritoneal access with flexible endoscope was obtained under the lifting of stomach wall using a double-straight needle device. Transgastric endoscope easily visualized the abdominal cavity in all directions. The closure of gastric orifice was performed by the hand-sewn technique using the thread for gastric wall lifting. Although the contamination of gastric contents might have occurred during transgastric

子宮内胎児鏡下手術のための 細径屈曲鉗子マニピュレータに関する研究

山下 紘正¹, 松宮 潔¹, 正宗 賢¹, 廖 洪恩², 千葉 敏雄³, 土肥 健純¹

東京大学大学院情報理工学系研究科¹

東京大学大学院工学系研究科²

国立成育医療センター特殊診療部³

Miniature bending forceps manipulator for intrauterine fetal surgery

Hiromasa YAMASHITA¹, Kiyoshi MATSUMIYA¹, Ken MASAMUNE², Hongen LIAO², Toshio CHIBA³,
Takeyoshi DOHI¹

Graduate School of Information Science and Technology, The University of Tokyo¹

Graduate School of Engineering, The University of Tokyo²

Department of Strategic Medicine, National Center for Child Health and Development³

1. 背景

脊髄髄膜瘤を始めとする胎児疾患には妊娠 19～25 週における子宮内外科治療が有効だが、術具の挿入方向は母体の胎盤位置によって大幅に制限されてしまい、非常に難易度の高い手術となる。術具の挿入位置に依らない柔軟なアプローチの実現には、従来の直線状の術具先端に多自由度を付加することが挙げられるが、子宮内手術で使用可能な術具の外径は 2～4mm と非常に細く、子宮外から柔軟に、かつ確実に操作できる自由度の追加には特別な機構が必要となる。そこで本研究ではリンク機構とワイヤ機構を組み合わせた新たな駆動方式を導入することで、中心に内径 0.8mm のチャンネルを有する外径 3.5mm のサイズに、1 自由度あたり±90° の屈曲 2 自由度を備え、先端部に鉗子機能を搭載した屈曲鉗子マニピュレータの開発を目的とする。

2. 方法

本マニピュレータは、リンク・ワイヤ駆動方式による 2 自由度屈曲機構²⁾とワイヤ駆動式鉗子機能を有する多自由度エンドエフェクタ (図 1)、屈曲機構駆動用のアクチュエータを搭載した直動ユニット、屈曲操作用のジョイスティックと鉗子操作用のグリップを有するインタフェース、そしてアクチュエータ制御用計算機から構成される (図 2)。屈曲機構の先端に搭載した鉗子部は屈曲部分から着脱可能であり、2 つのブレード形状を変更することにより、把持鉗子や剥離鉗子、剪刀などに交換可能である。

3. 結果

屈曲機構の性能評価実験では、根元側自由度で最大 150.1°、先端側自由度で最大 111.9° の駆動範囲を確認した。マニピュレータ先端の把持中心位置におけるばらつきは 0.8 mm 以下であり、最高で誤差 0.2 mm の高精度な屈曲駆動が可能であった。把持中心で測定した屈曲力は最大 2.57 N であり、また、鉗子機能における把持力は最大 3.48 N であった。

4. まとめ

リンク駆動とワイヤ駆動を組み合わせた 2 自由度屈曲鉗子マニピュレータを開発した。先端側屈曲自由度では若干駆動範囲が狭く、動力伝達の面で改善が必要だが、屈曲再現性はいずれの自由度でも高く、精度の高い操作が可能である。今後は動物実験を中心に、臨床における屈曲・把持性能の妥当性評価を進めていく。

本研究の一部は平成 17 年度厚生労働科学研究費補助金 (身体機能解析・補助・代替機器開発研究事業, H17-フィジ:006) 」、平成 17 年度科学研究費補助金 (基盤研究 (S)) 並びに日本学術振興会特別研究員制度の支援を受けている。

参考文献

- [1] Bianchi, D. W., et al., Fetology: diagnosis & management of the fetal patient, 東京, 南山堂, 2002.
[2] 山下紘正, 他, 胎児外科手術用多自由度屈曲マニピュレータの開発, 第 14 回日本コンピュータ外科学会大会論文集, pp239-240, 千葉, Nov, 2005.

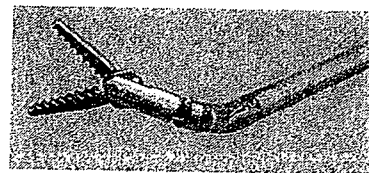


図 1 2 自由度屈曲鉗子先端部

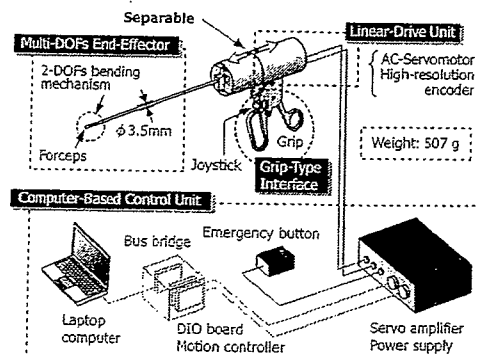


図 2 屈曲鉗子マニピュレータシステム構成

Miniature bending manipulator for fetoscopic intrauterine laser therapy to treat twin-to-twin transfusion syndrome

H. Yamashita · K. Matsumiya · K. Masamune ·
H. Liao · T. Chiba · T. Dohi

© Springer Science+Business Media, LLC 2007

Abstract

Background Recent typical therapy for twin-to-twin transfusion syndrome (TTTS) is selective laser photocoagulation of anastomotic communicating vessels on the placenta using the fetoscopic approach. The difficulty of a conventional laser device approach for this procedure depends significantly on the placental location, so a new robotized device is required to bend the direction of laser irradiation flexibly within the narrow uterus.

Methods The authors designed a miniature bending mechanism impelled by a wire-guided linkage driving method that provides a stable procedure for bending laser irradiation from -90° to 90° . Using this bending mechanism, the authors developed a bending manipulator with a diameter of 3.5 mm and a hollow central channel with a diameter of 0.8 mm for passing a glass fiber for neodymium:yttrium–aluminum–garnet (Nd:YAG) laser photocoagulation. The bending mechanism is motorized by an electrical actuator and controlled by a grip-type interface with a small joystick. The robotized tip's part and the

actuator's part are easily separable for cleaning and sterilization.

Results In performance evaluations of the manipulator, the bending characteristics with a glass fiber were examined. The bending range was -52.6° to 80° , with a very small hysteresis error, and the bending repeatability error was $0.5^\circ \pm 0.2^\circ$, which corresponds with the high accuracy of 0.2 ± 0.1 -mm positioning error at the glass fiber's tip. In the evaluation of Nd:YAG laser photocoagulation, the study confirmed that the manipulator performed effective laser photocoagulation of the placental phantom surface (underwater chicken liver). The large bending range, reaching 80° , enabled a flexible approach from various directions with a high irradiation efficiency of no less than 96.6%.

Conclusions The authors' original miniature bending manipulator can change the laser irradiating direction with highly repeatable positioning accuracy for speedy, safe, and effective vessel occlusion in clinical practice.

Keywords Miniature bending manipulator · Selective laser photocoagulation · Twin-to-twin transfusion syndrome

H. Yamashita (✉) · K. Matsumiya · K. Masamune ·
T. Dohi

Department of Mechano-Informatics, Graduate School of
Information Science and Technology, The University of Tokyo,
7-3-1, Hongo, Bunkyo-ku, Tokyo 113-8656, Japan
e-mail: hiromasa@atre.t.u-tokyo.ac.jp

H. Liao

Department of Precision Engineering, Graduate School of
Engineering, The University of Tokyo, 7-3-1, Hongo,
Bunkyo-ku, Tokyo 113-8656, Japan

T. Chiba

Department of Strategic Medicine, National Center for Child
Health and Development, 2-10-1, Okura, Setagaya-ku,
Tokyo 157-8535, Japan

Fetal surgery is performed on the fetus after approximately 19 to 25 weeks of pregnancy. The purpose is to treat fetal and placental morphologic defects, which can be diagnosed early before birth via relatively simple surgical procedures, allowing arrest of their progressions to severe states. Conventionally ex utero intrapartum treatment procedures (EXIT) are popular. However, possibilities of infection, complication, premature birth, and membrane rupture are high, and the outcomes are poor. On the other hand, recent progress in endoscopic surgery enables minimally invasive fetoscopic intrauterine surgery [4].

In fetoscopic surgery, therapy for twin-to-twin transfusion syndrome (TTTS) is particularly being confirmed in its effectiveness. This syndrome occurs in 10% to 15% of monochorionic twin gestations. It is caused by circulatory anastomoses and results in a higher rate of imbalance in the blood volume between recipient and donor twins. In severely affected cases, this syndrome is likely to be associated with high perinatal mortality or postnatal lifelong handicap [5].

For the recent therapy, selective endoscopic laser photocoagulation of anastomotic communicating vessels has been widely accepted as a more effective procedure [8, 9]. However, the fetoscopic approach must avoid any contact with the placenta, so the outcome of this procedure is significantly dependent on the placental location. Any contacts with the placenta cause heavy bleeding. Therefore, if the placenta is on the anterior abdominal wall side, the conventional straight-shape tool is not the approach for photocoagulation of vessels.

For the solution to this issue, bending instruments robotized to bend their tip's part are required for a safe and effective approach to target vessels (Fig. 1). Furthermore, to make invasion of the delicate uterine wall as minimal as possible, the diameter of the instruments must be minimized.

This study aimed to develop a miniature bending manipulator 3.5 mm in diameter with a robotized tip's part enabling highly accurate fetoscopic laser photocoagulation of anastomotic communicating vessels on the placenta, and to analyze bending characteristics and neodymium:yttrium-aluminum-garnet (Nd:YAG) laser photocoagulation using a placental phantom model to confirm safe and effective TTTS therapy.

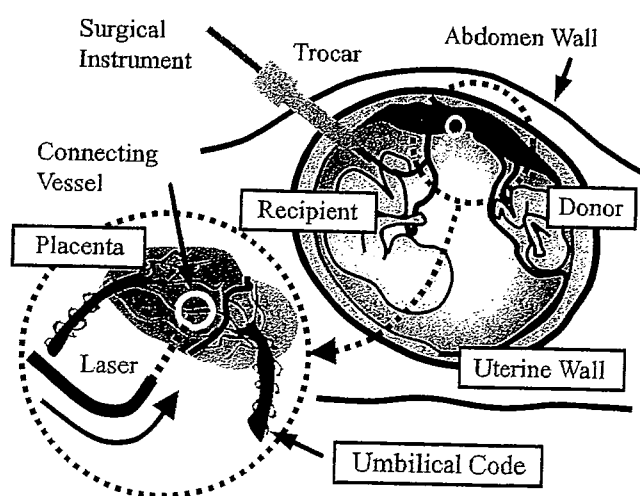


Fig. 1 Selective laser photocoagulation of anastomotic communicating vessels on the placenta for twin-to-twin transfusion syndrome (TTTS) therapy. If the placenta is on the anterior abdominal wall side, the bending instrument is required to change laser irradiating direction flexibly making no contacts with the placenta

Materials and methods

Bending mechanism

We designed a miniature bending mechanism including a central hollow channel for passage of a laser glass fiber. This mechanism is a fingerlike multijoint structure consisting of three frames and two joints based on the multi-slider linkage mechanism for the laparoscopic forceps manipulator [10, 11]. As shown in Fig. 2, tip-side frame 1 and base-side frame 3 are in contact with each other at both arc parts and joined by intermediate frame 2, which is driven by a pushing-pulling linear motion of the linkage. Moreover, frames 1 and 3 are connected by a pair of wire ropes (wire ropes A and B) that cross at the contact point to enable slipless smooth bending motion between the two frames, from -90° to 90° . Unlike a recently reported wire-driven manipulator [1, 3, 6], the pair of wire ropes in our method does not slide against the rotation of the frames and has a low risk of wear and tear caused by repeated or powerful manipulations.

Miniature manipulator

We developed a bending manipulator 3.5 mm in diameter with a robotized tip's part, including a central hollow channel 0.8 mm in diameter. The system configuration of the manipulator is shown in Fig. 3.

This system consists of five parts. The first part is the bending end-effector with a glass fiber (E-4070-B; Dornier MedTech, Tokyo, Japan) for Nd:YAG laser photocoagulation (Fig. 4). The diameter of the fiber is 0.7 mm, including the 0.4-mm core part. The constituent materials of the bending mechanism all are stainless steel (SUS304 and SUS316). The second part is the linear drive unit with a high-resolution AC-servomotor that enables highly accurate linkage driving. The third part is the handheld grip-type interface to be used like a conventional endoscopic surgical instrument. In this interface, we equipped a little joystick for easy bending control. The fourth part is the computer-based control unit, which calculates displacement of the sliding linkage by control from the joystick. The final part is the Nd:YAG laser photocoagulator (Dornier Medilas fibertom 5100; Dornier MedTech, Tokyo, Japan), which can detect candescent light during ablation of tissue to correct laser output energy against a set value. The bending end-effector is easily separated from the linear drive unit for cleaning and sterilization.

The total weight of the manipulator is 507 g. It has no cables, allowing easy and flexible maneuverability for fine intrauterine fetus surgery. Surgeons can operate the manipulator's bending angle from a joystick and can rotate the whole manipulator around the frames' central axis. The

Fig. 2 The concept of the bending mechanism driven by a wire-guided linkage driving method. Frames 1 and 3 are in contact with each other at both arc parts and joined by intermediate frame 2, which is driven by a simple sliding motion of the linkage. Frames 1 and 3 also are connected by wire ropes A and B to enable slipless bending motion between the two frames, from -90° to 90°

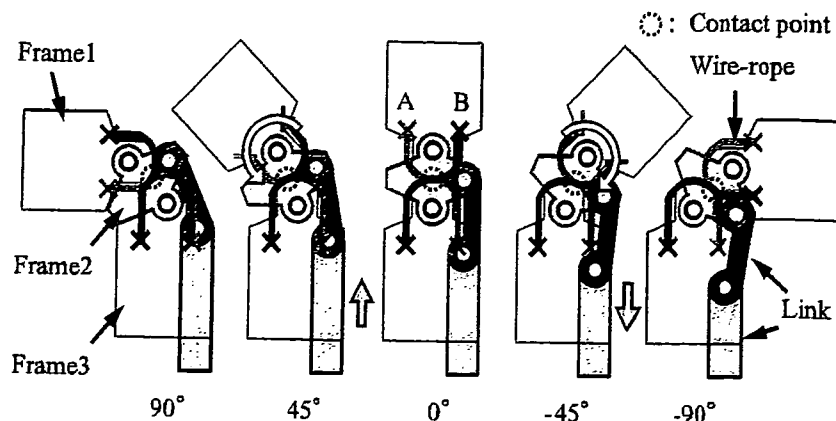
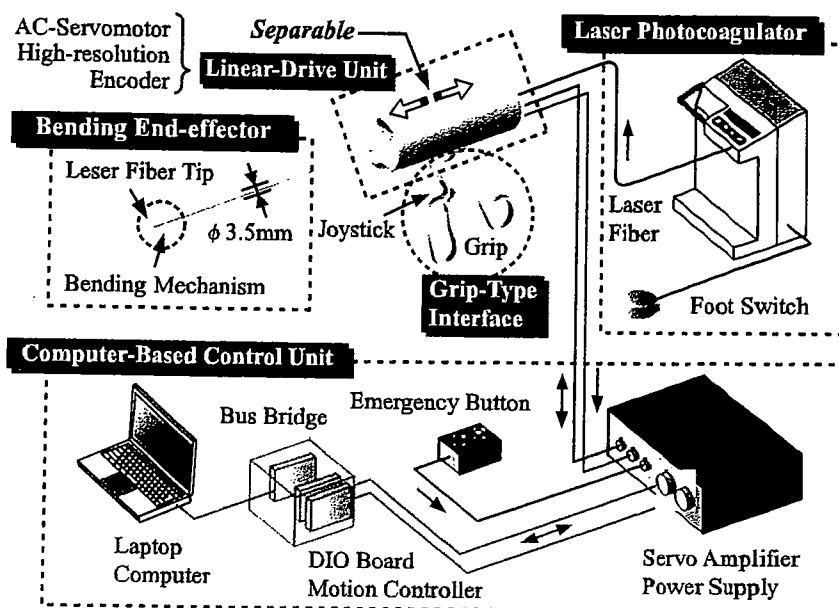


Fig. 3 The system configuration of the miniature bending manipulator consists of the bending end effector with a bending mechanism and a glass fiber, the linear drive unit with a high-resolution AC-servomotor that enables highly accurate linkage driving, the handheld grip-type interface for controlling bending angle, the computer-based control unit for calculating linkage sliding displacement, and the neodymium:yttrium-aluminum-garnet (Nd:YAG) laser photocoagulator



workspace of the manipulator's laser fiber tip is large and hemi-ellipsoidal, as shown in Fig. 5.

repeatability error, tip's part positioning accuracy, and hysteresis error are presented in Table 1.

Results

Performance evaluations

First, we examined the bending characteristics of the manipulator such as bending range, bending repeatability, tip's part positioning accuracy, and hysteresis error of the manipulator with or without a laser glass fiber. We changed the bending angle in steps of 10° : from 90° to 0° to -90° , and finally returning to 90° , repeating the steps five times. The bending angles were measured by an optical measurement instrument (FinePix F11; FUJIFILM Corporation, Tokyo, Japan) that had no distortion and a high resolution of 0.07 mm. The results of the hysteresis curve are shown in Fig. 6, and the measurement values of bending range, bending



Fig. 4 The bending manipulator tip with a glass fiber through the central channel for neodymium:yttrium-aluminum-garnet (Nd:YAG) laser photocoagulation

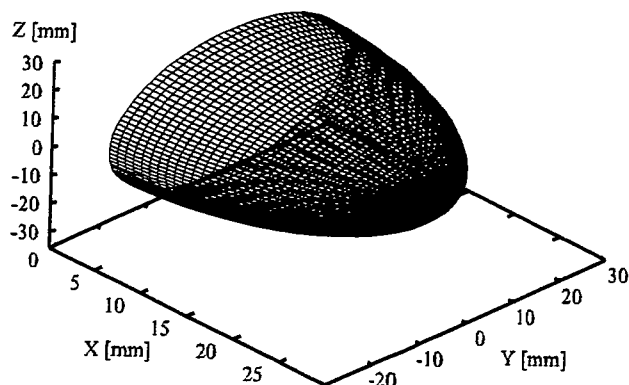


Fig. 5 The workspace of the manipulator's laser fiber tip with motorized bending motion and manual rotational motion. The workspace of the tip is large and hemi-ellipsoidal

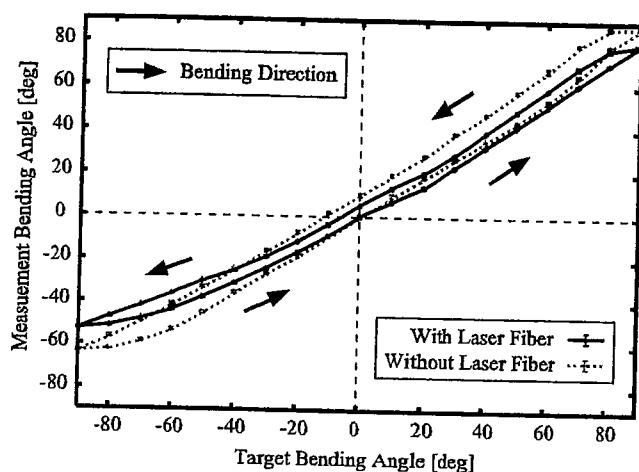


Fig. 6 Results of the manipulator's bending hysteresis curves measured by an optical instrument with and without a laser fiber, which is the relationship between the target bending angle and the measurement bending angle. The target bending angle is changed in 10° steps: from 90° to 0° to -90° , and then returning to 90° , with the steps repeated five times

Additionally, we examined the bending forces and torques with a laser glass fiber using a digital force gauge (FGP-2; NIDEC-SHIMPO Corporation, Kyoto, Japan), the resolution of which was 0.01 N. These results are shown in Table 2.

We measured output energy from the glass fiber tip's part with bending motion using a laser power meter

Table 1 Characteristics of the manipulator's bending motion measured by an optical instrument ($n = 5$)

Measurement item	With fiber	Without fiber
Bending range ($^\circ$)	-52.6 to 80	-63 to 88
Bending repeatability error ($^\circ$)	0.5 ± 0.2	0.5 ± 0.2
Tip's part positioning accuracy (mm)	0.2 ± 0.1	0.2 ± 0.1
Hysteresis error ($^\circ$)	<7.6	<14.5

Table 2 Bending forces and torques measured by a digital force gauge at the tip's part of the manipulator with a laser fiber ($n = 10$)^a

Direction ($^\circ$)	Bending force (N)	Bending torque (Nmm)
0 to 90°	1.56	20.6
0 to -90°	1.03	13.6

^a Neodymium:yttrium-aluminum-garnet (Nd:YAG) laser photocoagulation

(Power/Energy Meter Heads 30(150)A-HE; OPHIR Japan Co., Ltd., Saitama, Japan). The efficiency of Nd:YAG laser irradiation was no less than 96.6% despite the large bending angle reaching 80° , as compared with the irradiation with a straight shape (0°).

Next in the phantom experiment, we evaluated the feasibility of Nd:YAG laser photocoagulation of protein using the manipulator's various bending motions in a near clinical setting. The irradiation setting was 1 s at 50 W of power. In practical TTTS laser therapy, the irradiation condition determines the feasibility of vessel occlusion. The maximum diameter of the vessels to be ablated generally is less than 2 mm, and most importantly, the clinician should avoid the rapid heating of vessels using high-output laser energy. That is quite likely to cause an abrupt rise in blood temperature and intravascular vapor pressure with resultant rupture of the targeted vessels.

To arrange an embryonic environment, we set an underwater chicken liver as a phantom model to resemble an intrauterine placental surface. We used 1-DOF bending motion with hand-operated rotation around the central axis of the frames, assuming photocoagulation of the placental vessels in the narrow uterine environment. As shown in Fig. 7, we ablated the phantom surface from various directions with the manipulator's tip bent up to 80° .

Discussion

The manipulator with its laser glass fiber achieved high bending repeatability with less than 0.7° of error and high accuracy with less than 0.3-mm positioning error at the fiber tip. These results are sufficient for clinical laser photocoagulation of placental anastomotic connecting vessels, the diameters of which are approximately 1 mm.

The bending torque was sufficient for a large bending range reaching 80° , with a minimum bending radius of 4.2 mm. However, performance for bending in a minus direction was a little lower than that for bending in a plus direction. The cause of these results was asymmetry of the linkage's trajectory between the plus direction (pushing linkage) and the minus direction (pulling linkage). The relationship between the bending angle and the linkage displacement was not completely linear. Therefore, varia-

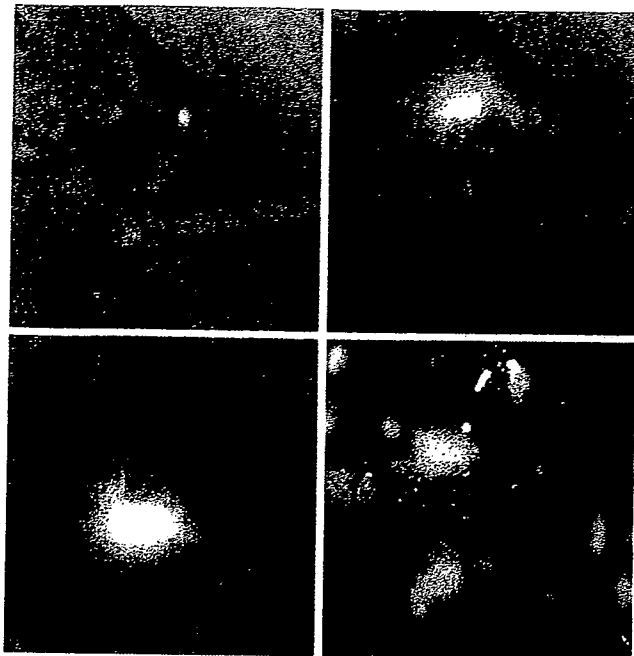


Fig. 7 Laser ablation test with underwater placental phantom model. **A** Guide light irradiation. **B** and **C** Neodymium:yttrium-aluminum-garnet (Nd:YAG) laser photocoagulations of the placental phantom model surface with bending motion of the manipulator. **D** Macro view of laser-ablated spots

tions in bending characteristics arose. The bending range with a fiber was a little less than without a glass fiber because of a fiber's restoring force. However, this difference was so small as not to affect bending maneuverability.

In the phantom experiment with a near clinical setting, we confirmed the high efficiency of laser irradiation in coagulating underwater protein without any loss of Nd:YAG laser photocoagulation energy despite a maximum bending angle of 80°. However, in clinical use, it is significant to keep a suitable distance between the manipulator's tip and the targeted vessels because they bleed easily. Generally, intraoperative hemorrhages from the placenta or placental vessels are likely to cease within minutes. Then it is possible to replace the bloody amniotic fluid partially with clear warm saline to complete the procedure even with our new system. If the hemorrhage seems massive and critical, the closed endoscopic procedure can be immediately converted into an open hysterotomy procedure.

Compared with conventional endoscopic robotic systems, as typified by the Endo Wrist of the da Vinci Surgical System (Intuitive Surgical, Inc., Sunnyvale, CA, USA), our system was superior in miniaturization and bending precision for minimally invasive intrauterine fetoscopic surgery. The especially suitable combination of wire and linkage mechanisms realized a more accurate bending manipulation and a larger bending range for its compact size than typical linkage-driven manipulators used for

endoscopic surgery [2, 7]. With regard to practical application of the system, commercial manufacturing is quite promising and certain considering its mechanically simple design and the need for universal clinical use.

Conclusion

Our original bending laser manipulator has a small diameter of 3.5 mm and is applicable for intrauterine fetal surgery. It avoids excessive damage to the uterine wall and can change the direction of Nd:YAG laser irradiation flexibly with highly repeatable positioning accuracy. In clinical practice, the manipulator enables speedy and efficient vessel occlusion without invasion to the placenta, fetus, or amniotic membrane within the narrow uterus.

Acknowledgments A part of this work was supported by Health and Labour Sciences Research Grants in 2005 (research on medical devices for analyzing, supporting, and substituting the function of human body; H17-Physi-006), by FY2005 JSPS Grants-in-Aid for Scientific Research Development of Next Generation End Effector and Navigation System for Computer Aided Surgery (17100008), and by Research Fellowships of the Japan Society for the Promotion of Science for Young Scientists (04140000227).

References

1. Abbou CC, Hoznek A, Salomon L, Olsson LE, Lobontiu A, Saint F, Cicco A, Antiphon P, Chopin D (2001) Laparoscopic radical prostatectomy with a remote controlled robot. *Urology* 165: 1964–1966
2. Arata J, Mitsuishi M, Warisawa S, Tanaka K, Yoshizawa T, Hashizume M (2005) Development of a dexterous minimally-invasive surgical system with augmented force feedback capability. *Proceedings of the 2005 IEEE/RSJ International Conference on Intelligent Robots and Systems*, pp 3207–3212
3. Dario P, Carrozza MC, Marcacci M, D'Attanasio S, Magnani B, Tonet O, Megali G (2000) A novel mechatronic tool for computer-assisted arthroscopy. *IEEE Trans Inform Technol Biomed* 4: 15–28
4. Evans MI, Adzick NS, Holzgreve W, Harrison MR (2001) *The unborn patient: the art and science of fetal therapy*, 3rd ed. Saunders, Philadelphia
5. Feldstein VA, Machin GA, Albanese CT, Sandberg P, Farrell JA, Farmer DL, Harrison MR (2000) Twin-twin transfusion syndrome: the "select" procedure. *Fetal Diagn Ther* 15: 257–261
6. Ikuta K, Sasaki K, Yamamoto K, Shimada T (2002) Remote microsurgery system for deep and narrow space: development of new surgical procedure and microrobotic tool. *Proceedings of the 5th International Conference on Medical Image Computing and Computer-Assisted Intervention*, pp 163–172
7. Peirs J, Reynaerts D, Van Brussel H (2001) A miniature manipulator for integration in a self-propelling endoscope. *Sens Actuators A*: 343–349
8. Quintero RA, Comas C, Bornick PW, Allen MH, Kruger M (2000) Selective versus nonselective laser photocoagulation of placental vessels in twin-to-twin transfusion syndrome. *Ultrasound Obstet Gynecol* 16: 230–236
9. Senat MV, Deprest J, Boulvain M, Paupe A, Winer N, Ville Y (2004) Endoscopic laser surgery versus serial amnioreduction for

- severe twin-to-twin transfusion syndrome. *N Engl J Med.* 351: 136–144
10. Yamashita H, Hata N, Hashizume M, Dohi T (2004) Handheld laparoscopic forceps manipulator using multislidder linkage mechanisms. *Lect Notes Computer Sci* 3217: 121–128
 11. Yamashita H, Kim D, Hata N, Dohi T (2003) Multislidder linkage mechanism for endoscopic forceps manipulator. *Proceedings of the 2003 IEEE/RSJ International Conference on Intelligent Robots and Systems*, pp 2577–2582

1505 平面型マイクロコイルを用いた局所高分解能MRIに関する研究

Local High Resolution MRI with a Micro Planar Coil

○土肥 徹次 (東京大) 高橋 英俊 (東京大)

桑名 健太 (東京大) 正 松本 潔 (東京大)

正 下山 勲 (東京大)

Tetsuji DOHI, The University of Tokyo, 7-3-1 Hongo, Bunkyo-ku, Tokyo

Hidetoshi TAKAHASHI, The University of Tokyo

Kenta KUWANA, The University of Tokyo

Kiyoshi MATSUMOTO, The University of Tokyo

Isao SHIMOYAMA, The University of Tokyo

This paper reports on a micro planar coil as a receiver for a high resolution MRI (Magnetic Resonance Imaging). In this study, a micro planar coil of 10 mm in diameter was fabricated. The MRI signal receiving device was made by attaching the micro coils to the tip of acrylic pipes. The signal to noise ratio of MR image taken by the micro planar coil was 8 times as high as MR image taken by medical MRI coil. MR images of okra (*Abelmoschus esculentus*) were acquired with $2.0 \times 2.0 \times 2.0 \text{ mm}^3$ and $0.5 \times 0.5 \times 1.0 \text{ mm}^3$ resolutions.

Key Words: MRI, micro planar coil, S/N ratio, high sensitivity.

1. 背景・目的

医療用MRIは、侵襲性が非常に低く、X線CT (Computed Tomography)では撮像が困難な軟部組織を高いコントラストで撮像可能であるため、非侵襲的な診断装置として幅広く利用されている。また、近年では、手術中に利用することで腫瘍の取り除きをできるだけ少なくし、手術成績の向上に利用しようという研究も行われている。しかし、一方で計測時間が長く、空間分解能もサブミリから数ミリオーダーであるため、計測時間の短縮および空間分解能の向上が期待されてきた。この計測時間の短縮と空間分解能の向上に対して、MRI受信信号のS/N比を向上させることが効果的な解決策である。

そこで、本研究ではMRI信号のS/N比向上のための高感度なMRI信号受信コイルとして、MEMS (Micro Electro Mechanical Systems) 技術を利用した平面型マイクロコイルを試作する。MEMS技術を利用した平面型マイクロコイルは、その感度領域をコイル近傍に集中させることができるため、感度領域は狭いが非常に高い感度でのMRI信号計測が可能となる。この平面型マイクロコイルをカテーテルや内視鏡の先端部に配置 (Fig. 1) し、術中MRIのための新しい術具としての有効性を示すことが本研究の目的である。

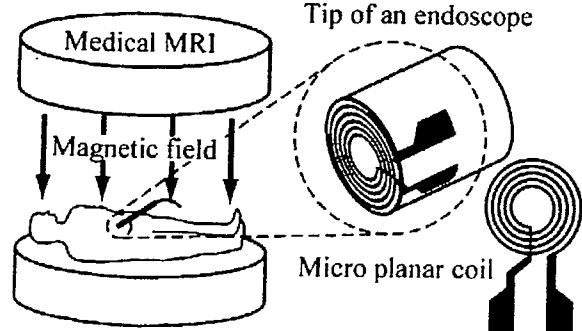


Fig. 1 Concept of a micro planar coil. The micro planar coil is located at the tip of a catheter or an endoscope.

これまで、MEMS技術を利用した小型かつ高感度なコイルによって、MRI信号受信デバイスの試作が行われてきた。マイクロサイズのコイルを利用することで分解能 $16 \times 23 \times 100 \mu\text{m}^3$ での画像計測^[1]や、マイクロ流路と組み合わせた高感度なNMR分光法の研究が行われてきた^[2]。我々も直径5 mmおよび20 mmの平面型MEMSコイルをアクリルパイプの先端に搭載することで、0.2 Tという低い静磁場であるにもかかわらず、分解能 $0.5 \times 0.5 \times 1.0 \text{ mm}^3$ での高分解能画像計測を実現した^[3]。これに対して本研究は、これらのマイクロコイルを利用したデバイスが、術中MRIで利用する新しい術具として有効であることを示すことが目的である。そのため、内視鏡先端部をマイクロコイルを用いたデバイスと置き換え、他の術具と同様に利用できるデバイスを実現する。

2. 平面型マイクロコイルの試作と特性計測

平面型マイクロコイルの試作プロセスをFig. 2に示す。試作したコイルには、MRI画像計測に与える影響が少ないCuやTi、ポリイミドを材料として利用した^[4]。試作プロセスは、Cu/ポリイミドのフレキシブル基板を利用した。はじめに、基板のポリイミド面側にコイルのワイヤ部となるTi層とCu層を蒸着装置により成膜する。Ti/Cu層をコイル形状にパターンニングした後、ワイヤ部の厚さを増加させ、抵抗値を減少させるためにCuメッキを行った。この際、フォトレジストの側壁を利用することで線幅が変化しないようにした。最後に、裏面のCu層をパターンニングしてコイル中心部と外部接続用電極を配線し、コイルを基板から切り離すことで、平面型マイクロコイルが完成する。

試作した平面型マイクロコイルの写真とその電気的特性をFig. 3に示す。コイルは、直径10 mm、線幅、線間隔ともに100 μm 、巻き数は16である。試作したコイルは、静磁場強度が0.2 TのMRIで利用するため、

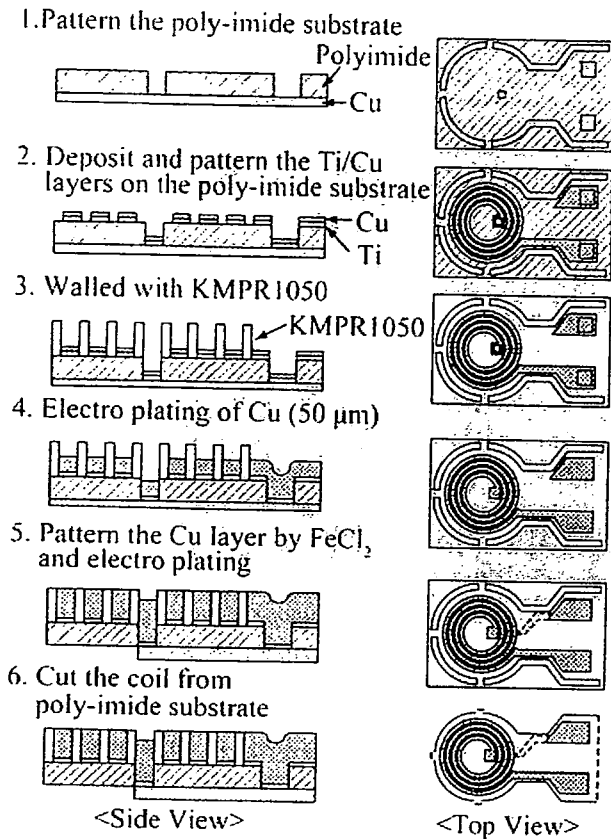


Fig. 2 Fabrication process of a micro planar coil.

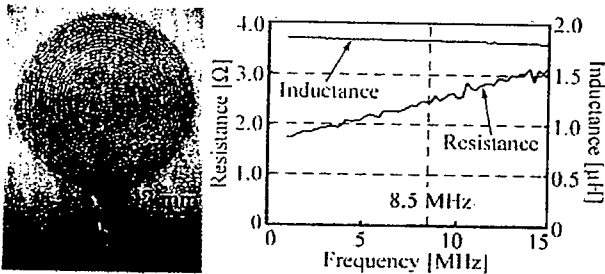


Fig. 3 Photographs of the fabricated micro planar coil. The diameter of the coil is 10.0 mm. The resistance and inductance of the coil are 2.5 Ω, and 1.8 μH at 8.5MHz, respectively.

周波数8.5 MHzで高い特性を持つように設計した。Fig. 3の基礎特性計測結果より、試作したコイルは、周波数8.5 MHzにおいて抵抗値 2.5 Ω, インダクタンス1.8 μHであり、0.2 TのMRI用受信コイルとして十分な特性を持っていることが確認できた。

3. MRI 信号受信回路の試作と画像計測

次に、試作したマイクロコイルをMRI信号受信回路と組合せ、MRI信号受信デバイスとした。Fig. 4に示すように、MRI信号受信回路は平面型マイクロコイルのインピーダンスと周波数を調整するための可変コンデンサと、MRI装置と接続するための保護回路からなる。

このMRI信号受信回路をアクリルパイプの側部に配置し、平面型マイクロコイルを先端部に配置した。

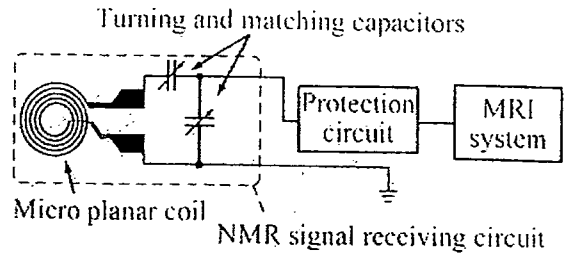


Fig. 4 Schematics of MRI signal receiving circuit.

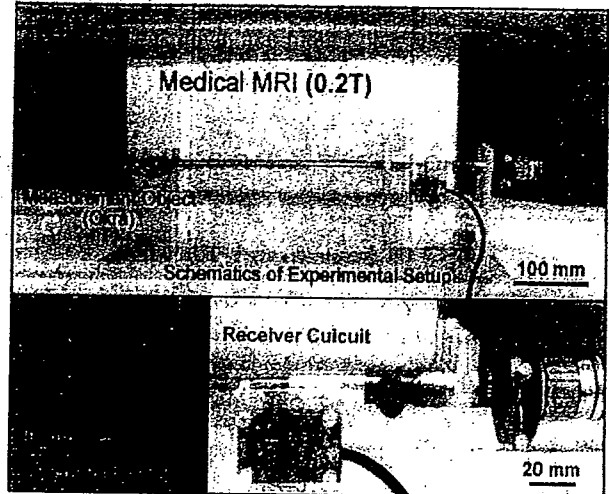


Fig. 5 photographs of the MRI signal receiver with micro planar coil. The planar coil is placed at the tip of acrylic pipe with the receiving circuit. The acrylic pipe can be connected to the base of the endoscope.

Table 1 SNRs of MR images of the phantom..

	2.0×2.0×2.0 mm ³ resolution	0.5×0.5×1.0 mm ³ resolution
Medical Coil	30	3.7
5 mm Coil	259	28
10-mm Coil	258	19
20 mm Coil	264	13

アクリルパイプは直径がφ11 mmであり、内視鏡の根元部と接続可能とした。試作したデバイスをFig. 5に示す。本研究では、φ10 mmの腹腔鏡の根元部を利用したが、MRI対応内視鏡と接続すれば、内視鏡画像と同時にMRI画像を取得可能なデバイスとなる。

試作したMRI信号受信デバイスの特性評価のために、MRI信号のS/N比計測を行った。計測結果をTable. 1に示す。S/N比計測では、水をファントムとして利用し、分解能、2.0×2.0×2.0 mm³, 0.5×0.5×1.0 mm³の画像計測を行った。この際、比較として、φ200 mm程度の医療用コイル、直径5 mmと直径20 mmの平面型マイクロコイル^[3]を利用した。Table. 1の計測結果より、試作したφ10 mmの平面型マイクロコイルを用いたMRI信号受信デバイスは、従来の医療用コイルと比較して5~8倍程度の高い受信感度を持っていることがわかった。

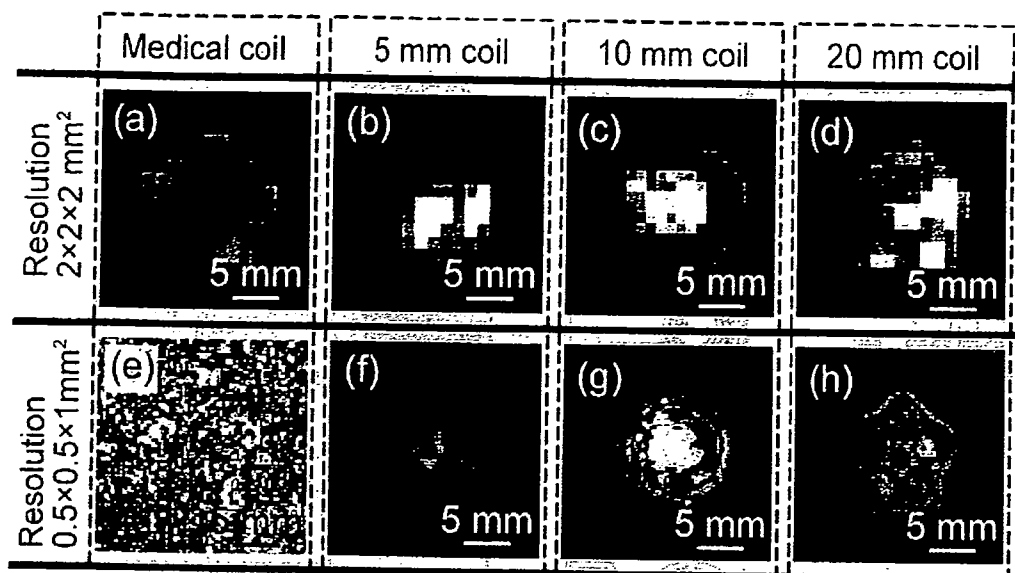


Fig. 7 MR images of an okra taken by the micro planar coils and medical coil. The resolutions of the images were (a - d) $2.0 \times 2.0 \times 2.0 \text{ mm}^3$ and (e - h) $0.5 \times 0.5 \times 1.0 \text{ mm}^3$. The internal structure of an okra can be observed.

最後に、この受信デバイスを MRI 装置に接続し、Fig. 6 に示すようにオクラの断層画像計測を行った。Fig. 6 (a)~(d)は分解能 $2.0 \times 2.0 \times 2.0 \text{ mm}^3$ で計測した MRI 画像であり、Fig. 6 (e)~(h) は分解能 $0.5 \times 0.5 \times 1.0 \text{ mm}^3$ で計測した MRI 画像である。Fig. 6 より、試作した平面型マイクロコイルは、従来の医療用コイルと比較して高い S/N 比で画像取得可能であることがわかる。そのため、従来の医療用コイルでは撮影が困難であった分解能 $0.5 \times 0.5 \times 1.0 \text{ mm}^3$ の条件でも、感度分布が不均一ではあるが、画像取得可能であることがわかった。また、試作した MRI 信号受信デバイスは、硬性内視鏡の根元部を含むが、他の平面型マイクロコイルを用いた画像計測と同程度の画質で画像取得が可能であり、術中 MRI で利用する新しい術具として有効であることが確認された。

4. 結論

本研究では MEMS 技術を利用し、感度領域が局所的だが、非常に高感度な MRI 信号受信コイルを試作した。φ11 mm の円筒形アクリルパイプの先端に試作した平面型マイクロコイルを配置し、コイルの S/N 比を計測した。その結果、試作したマイクロコイルは、従来の医療用 MRI コイルと比較して、5~8 倍の S/N 比を持ち、より高分解能な MRI 画像取得が可能であることを確認した。

参考文献

- [1] H. Wensink et al., "High signal to noise ratio in low field NMR on chip, simulation and experimental results," Proc. of 17th IEEE MEMS, pp. 407-410, 2004.
- [2] C. Massin et al., "Planer microcoil-based magnetic resonance imaging of cells," Proc. of 13th International Conference on Solid-State Sensors, Actuators and Microsystems, pp. 967-970, 2003.
- [3] H. Takahashi et al., "A Micro Planar Coil for Local High Resolution Magnetic Resolution Imaging," Proc. of 17th IEEE MEMS, pp. 549-552, 2007.
- [4] D. Stoianovici, "Multi-imager compatible actuation principles in surgical robotics," Journal of Medical Robotics and Computer Assisted Surgery, vol. 1(2), pp. 86-100, 2005.